AU0019036

UMP 98/60

STRUCTURE OF LIGHT MASS (EXOTIC) NUCLEI AS EVIDENCED BY SCATTERING FROM HYDROGEN

K. Amos[(A)], P. J. Dortmans[(A)] , and S. Karataglidis[(B)]

[(A)] School of Physics, University of Melbourne, Parkville, Victoria 3052, Australia.
[(B)] TRIUMF, 4004 Wesbrook Mall, Vancouver, British Columbia, V6T 2A3, Canada.

Abstract: Microscopic optical model potentials generated by full folding of realistic two-nucleon (NN) interactions with nuclear structure specified by large basis shell model calculations have been constructed. With those (nonlocal) potentials, predictions of light mass nuclei–hydrogen scattering result that agree well with observations of cross sections and analyzing powers.

1 INTRODUCTION

A topic of current interest is the specification of the structures of exotic nuclei such as the neutron/proton rich isotopes of light mass nuclei. Many of these nuclei can be formed as radioactive beams and experiments made to determine their scattering from, and reactions with, stable nuclei. The scattering of such exotic nuclei from hydrogen targets is of particular interest as that scattering data should be sensitive to properties of the ground state of these nuclei. Analysis of that data is feasible also as inverse kinematics equates the process to the scattering of energetic protons from them as targets.

It is now possible to predict observables from elastic and inelastic proton-nucleus (pA) scattering at intermediate energies [1] in a manner consistent with that employed for electron scattering. To do so, three basic aspects of the system under investigation are required. Where possible, these properties must be determined independently of the pA scattering system being studied. First, the description of the nucleus (i.e. one body density matrix elements, OBDME) should be determined from large scale structure calculations which describe well the ground state properties (and low excitation spectra if pertinent) of the nucleus in question. The second aspect is the choice of nucleon bound state wave functions. They, with the given OBDME, can be assessed by their use in fitting elastic electron scattering form factors. The final ingredient is the complex, energy and density dependent, effective NN interaction that exists between the incident and struck nucleon. This effective interaction, which we suppose has central, tensor and two–body spin–orbit components each having a radial variation that is a sum of Yukawa functions, is defined so that it reproduces accurately (momentum space) half–off–shell NN t– and g–matrices associated with realistic NN potentials.

With all three ingredients specified, energy dependent, complex, and non-local optical potentials have been formed for the scattering of 65 to 800 MeV protons from any nucleus. With those nonlocal optical potential, solutions of the Schrödinger equations yield differential cross sections, analyzing powers and spin rotations for elastic scattering in very good agreement with data [1]. We stress that they are predictions. No *a posteriori* adjustment to any of the details of the calculations has been made.

The effective NN interaction in nuclei

We consider a realistic microscopic model of pA reactions to be one that is based upon NN t–matrices whose on–shell values are consistent with measured NN scattering data to and above the incident energies of interest, and whose properties off of the energy shell are consistent with data such as NN bremsstrahlung. For energies below the pion threshold, the Paris, Bonn, and Hamburg (OSBEP) interactions [2] satisfy those requirements quite well. Above that threshold, no meson exchange model accounts well enough for the resonances and flux loss effects to match the Arndt phase shifts. Recently, however, by supplementing the OBEP model interactions with NN optical potentials [3] those phase shifts could be matched to 2.5 GeV with (NN) optical potentials that are smooth functions of energy, and are consistent with both the known resonance characteristics and the known profile function of very high energy NN scattering. Such we have found to be appropriate starting interactions to determine effective NN interactions within the nuclear medium when energies are above the pion threshold when minimal relativity is considered.

Considering energies below pion threshold, the NN t–matrices are solutions of Lippmann–Schwinger equations. However, if the struck nucleon is embedded in a nuclear medium, calculations of the NA optical potential should be based instead upon medium modified NN g–matrices. We take those to be solutions of Brueckner–Bethe–Goldstone (BBG) equations in which allowance is made for Pauli blocking and average fields upon the scattering. Details of the calculations have been given previously [4]; the results being tables of complex numbers for each NN channel, for each incident energy, at each Fermi momentum value, and for a selected set of relative momenta.

At energies to over 200 MeV, the medium effects that differentiate the g- from the t-matrices are quite severe [4]. That is especially so for the on-shell values. Furthermore these effects are quite complex and cannot be represented at all reasonably in any simple function of the density itself.

The shell models of structure

For light mass nuclei ($A < 16$), all significant structure calculations have been made using the shell model program OXBASH [5]. With very light mass nuclei (such as the He and Li isotopes), in the main we have used the matrix elements of Zheng *et al.* [6] in those calculations. Complete $(0 + 2 + 4)\hbar\omega$ and also $(0+2+4+6+8)\hbar\omega$ model space calculations have been considered for $A \leq 6$. For $6 < A > 16$, complete $(0+2)\hbar\omega$ space calculations have been made using a standard (MK3W) set of potentials. The structure of exotic nuclei (^{6,8}He, ^{9,11}Li) have been determined in this way as well. More details of these shell model structures of light mass nuclei have been published recently [7]. The results of the calculations are OBDME, and, for the the most recent studies [6, 7], the single nucleon bound state wave functions.

The pA optical potentials

When effective interactions as described above are folded with the target OBDME and proper account taken of the antisymmetry of the the pA wave function, complex nonlocal spin dependent optical potentials result. They have the form

$$\begin{aligned} U(\vec{r}_1,\vec{r}_2;E) &= \delta(\vec{r}_1-\vec{r}_2)\sum_n \zeta_n \int \varphi_n^*(\vec{s})v^D(\vec{r}_{1s},E;\rho[k_f(r_{1s})])\varphi_n(\vec{s})\, d\vec{s} \\ &\qquad + \sum_n \zeta_n \varphi_n^*(\vec{r}_1)v^{Ex}(\vec{r}_{12},E;\rho[k_f(r_{12})])\varphi_n(\vec{r}_2) \\ &\Rightarrow U_D(\vec{r}_1,E) + U_{Ex}(\vec{r}_1,\vec{r}_2;E) \end{aligned}$$

where v^D and v^{Ex} are appropriate combinations of the NN ST channel elements of the effective interaction, $\varphi_j(\vec{r})$ are the single nucleon bound state wave functions and ζ_n are the shell occupancies of the target nucleus. In the past, the leading term has been used alone (the $g\rho$ or $t\rho$ approximation), or the nonlocal (exchange) elements have been approximated by 'equivalent' local interactions. Neither is a satisfactory approach for the analyses of data from the scattering of intermediate energy protons. Indeed when we used the $g\rho$ form with our effective interaction, the cross sections and analyzing powers that result are markedly changed from those given by our complete calculations and which reproduce observed results very well [1].

2 RESULTS OF CALCULATIONS

Using the complete, nonlocal optical potential generated microscopically as described above, we have made predictions of differential cross sections, analyzing powers, and spin rotations for the elastic scattering of 65 and 200 MeV protons from 50 nuclei ranging from ^{3}He to ^{238}U. All of those predictions are in very good agreement with observation for data forward of 60° scattering angle typically (for which cross sections are of order 1 mb/sr and greater).

Scattering from stable nuclei

Results of our calculations of proton scattering from many stable nuclei have been presented in detail elsewhere [1]. Herein to illustrate, sample results for 65 MeV from a set of nuclei (^{7}Li to ^{64}Zn) are given in Figs. 1 and 2 (cross sections and analyzing powers respectively). We stress that the calculated results presented are predictions; the data were included in these figures AFTER the curves shown were defined. For a complete discussion the reader is referred to the recent literature [1], wherein the crucial role of using an NN effective interaction in which appropriate account of medium modifications is explained.

Scattering of ^{6,8}He, and ^{9,11}Li from Hydrogen

The results from our analyses of proton scattering from ^{3,4}He and ^{6,7}Li [7] indicate that we have appropriate shell model descriptions of these light nuclei. Such shell models should be appropriate also for the exotic light mass nuclei. Indeed already the $(0+2)\hbar\omega$ model space structure has been used with success in studies of proton scattering from ^{9,11}Li [8]. Also, and very recently, the low excitation spectrum of ^{11}Li seems to have been identified [9] and, although no spin-parity assignments have yet been made, the negative parity states of our spectrum match likely entries from that experiment. For the other 'exotic' nuclei to be considered, ^{6,8}He, the $(0+2+4)\hbar\omega$ model space structure has been used. In fact the ground state of ^{6}He we take as the isobaric analogue of the $0^+;1$ (3.56 MeV) state in ^{6}Li. The structure calculations were made using the G matrix interaction of Zheng *et al.* as input to the shell model code OXBASH. Calculations that use single-particle wave functions from the shell model calculations do not coincide with a "halo" structure. We estimate the effects of an existent halo by varying those single particle wave functions. In all cases then we first specify the single particle bound states by Woods-Saxon (WS) wave functions. Those which gave good reproduction of the elastic electron scattering form factors of ^{6}Li were used for the ^{6,8}He calculations while those which reproduced the elastic electron scattering form factors of ^{9}Be were used in the calculations for ^{9}Li and ^{11}Li. With such wave functions, we consider the nuclei to be of "non–halo" type.

In these analyses, the ^{8}He and ^{9}Li results act as controls. Since the single neutron separation energies are 2.137 MeV and 4.063 MeV for ^{8}He and ^{9}Li, respectively, we consider ^{8}He to be an example of a neutron skin while ^{9}Li we believe is a simple core nucleus. We artificially ascribe a halo to these nuclei to ascertain if the procedure and data are sensitive enough to detect the flaw. To specify "halo" nuclear properties, we adjust the WS potentials such that the relevant neutron orbits are weakly bound. This guarantees an extensive neutron distribution. For ^{6,8}He, the 0p-shell binding energy was set to 2 MeV, which is close to the separation energy (1.87 MeV) of a single neutron from ^{6}He. For ^{9}Li and ^{11}Li, the halo was specified by setting the binding energy for the WS functions of the $0p_{\frac{1}{2}}$ and higher orbits to be 0.5 MeV. The neutron density profiles for ^{6}He, ^{8}He, ^{9}Li, and ^{11}Li obtained from the present shell model calculations are shown in Fig. 3. Therein the dashed and solid lines portray, respectively, the neutron profiles found with and without the halo conditions being implemented. The dot-dashed line in each case represents the proton density. As the folding process defines the optical potentials, we expect that the internal ($r < r_{\text{rms}}$) region influences the predictions of differential cross sections, notably at large scattering angles.

With the structures defined above, calculations in inverse kinematics were made of the scattering of 72 MeV per nucleon ^{6,8}He and of 60 - 62 MeV per nucleon ^{9,11}Li ions from hydrogen targets. The core single particle wave functions were those used in our calculations of scattering from the other He and Li isotopes. Now, however, there are more loosely bound neutrons and we have little data other than the scattering from hydrogen to help ascertain details of these. When the OBDME and wave functions discussed above were used in calculations of proton scattering, the differential cross sections that are compared with the data in Fig. 4 were obtained. The predictions obtained by using the no-halo (basic shell model) structure information are displayed by the solid curves, while those found by using the enforced neutron 'halo' forms are depicted by the dashed curves. Our results are very suggestive of a neutron 'halo' for ^{11}Li given that the match to data came with the $0p_{1/2}$, $1s$–$0d$, and the $0f$–$1p$ shell neutrons in the ground state being described by WS wave functions with 0.5 MeV binding energies. Likewise the comparisons indicate that ^{9}Li and ^{8}He do not have more extensive neutron distributions than the neutron skins that standard shell model calculations give.

It is of note that the halo nature of the nucleus is manifest in these differential cross sections at relatively large momentum transfer values. As such those cross sections are not particularly sensitive to the details of the wave function at the large radii (the traditional halo region). Thus the current scattering data reflect the 'depletion' (or no) of neutron strength in the interior of these nuclei from that we expect of non-halo constructs. At these energies, there are variations in cross section predictions caused dominantly by the neutron probability amplitudes at large radii. But they occur in the vicinity of the hadron–Coulomb interference regime. For 60 to 70A MeV light ions this is the region between 5 and 10° C. of M. scattering angle.

Scattering of 800 MeV protons from ^{12}C

Radioactive beams are planned at higher energies and our results [1] indicate that the microscopic model approach can be used with confidence at 200A MeV. We demonstrate next that such should also be the case at 800A MeV.

We have used boson exchange model NN interactions [2], OSBEP and BCC3 specifically, modulated by NN optical potentials [3], to specify NN t- (and g-) matrices at 800 MeV. With those t-matrices, the SM97 phase shifts to 2.5 GeV are fit extremely well. Coordinate space effective interaction forms that map very well the associated 800 MeV t– and g–matrices have been determined and then used in a full folding model to specify the complex and nonlocal optical potentials for 800 MeV protons incident on ^{12}C. The structure of the target used in that folding was determined from a large space (complete $(0 + 2)\hbar\omega$) shell model calculation which, in the past, gave electron scattering form factors in very good agreement with measured values. Thereby all quantities required in the folding process have been preset to make solution of the associated nonlocal pA Schrödinger equations predictive of the pA scattering phase shifts and so of the differential cross sections and analyzing powers. The differential cross section data from 800 MeV protons scattering off of ^{12}C are shown in Fig. 5. Clearly with just the basic OBEP used to specify our optical potentials (the left hand panel) neither result matches observation, although the BCC3 interaction gives better predictions than the OSBEP case. The BCC3 interaction accounts for effects of the Δ resonance and so innately is a 'more realistic' base interaction for the energy regime above 300 MeV. However, when either of the interactions are modulated by an (NN) optical potential and the proton-^{12}C optical potential defined by a full folding of the effective interactions specified by the attendant t- and g-matrices, our p$-^{12}$C cross section and analyzing power predictions are in very good agreement with the data to scattering angles of 25° (by which the magnitudes have fallen to less than 0.1 mb/sr). The effects of the modulation of both the OSBEP and the BCC3 models are very noticeable with the cross sections and even more so with the analyzing powers. Only with the modulations that tune OSBEP and BCC3 against the SM97 data set has satisfactory reproductions of that analyzing power structure been found.

3 CONCLUSIONS

Our predictive theory of $p - A$ scattering permits analyses of radioactive beam–hydrogen scattering to assess conjectured matter profiles of those exotic nuclei. We are confident that such is the case for all energies in the range 60A to 800A MeV. The available scattering data from hydrogen confirm that ^{11}Li is a halo nucleus, while the analysis of the scattering data correctly determines that both ^{8}He and ^{9}Li are not. The low-angle scattering results also suggest that ^{8}He is a neutron skin nucleus, as found from breakup reactions. The available scattering data for ^{6}He from hydrogen are not extensive enough to discriminate between the halo and non-halo scenarios; in the measured region they suggest for ^{6}He a very similar matter distribution compared to ^{6}Li.

References

[1] P. J. Dortmans, K. Amos, and S. Karataglidis, *J. Phys. G* **23**, 183 (1997); P. J. Dortmans, K. Amos, S. Karataglidis, and J. Raynal, *Phys. Rev. C* **58**, 2249 (1998).

[2] M. Lacombe *et al.*, *Phys. Rev. C* **21**, 861 (1980); R. Machleidt. *Adv. Nucl. Phys.* **19**, 189 (1989); L. Jäde and H.V. von Geramb, *Phys. Rev. C* **55**, 57 (1997); *ibid.* C **56**, 1218 (1998).

[3] H.V. von Geramb, K.A. Amos, H. Labes, and M. Sander, *Phys. Rev. C* **58**, 1948 (1998).

[4] P. J. Dortmans and K. Amos, *J. Phys.* **G17**, 901 (1991); *Phys. Rev C* **49**, 1309 (1994).

[5] B. A. Brown, A. Etchegoyen, and W. D. M. Rae, *computer code OXBASH-MSU*, MSUCL Report No. 524, 1986 (unpublished).

[6] D. C. Zheng *et al.*, *Phys. Rev. C* **52**, 2488 (1995).

[7] S. Karataglidis, B. A. Brown, P. J. Dortmans, and K. Amos, *Phys. Rev. C* **55**, 2723 (1997); P. J. Dortmans, K. Amos, and S. Karataglidis, *Phys. Rev. C* **57**, 2433 (1998).

[8] S. Karataglidis, P. G. Hansen, B. A. Brown, K. Amos, and P. J. Dortmans, *Phys. Rev. Lett.* **79**, 1447 (1997).

[9] M. G. Gornov, *et al.*, *Phys. Rev. Lett.* **81**, 4325 (1998).

Figure 1 The differential cross sections from the elastic scattering of 65 MeV protons from diverse nuclei

Figure 2 The analyzing powers from the elastic scattering of 65 MeV protons from diverse nuclei

Figure 3 The proton and neutron (non-halo and halo) density profiles of some exotic nuclei

Figure 4 The differential cross sections for the scattering of $72A$ MeV ^{6,8}He and of $62A$ MeV ^{9,11}Li from hydrogen.

Figure 5 Differential cross section and analyzing power of 800 MeV protons scattered from ^{12}C.

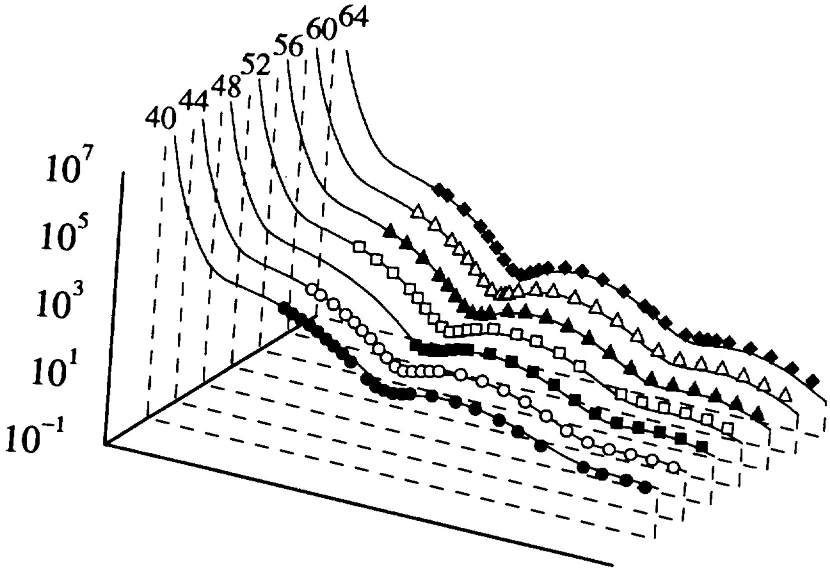

40 44 48 52 56 60 64
10^7
10^5
10^3
10^1
10^-1

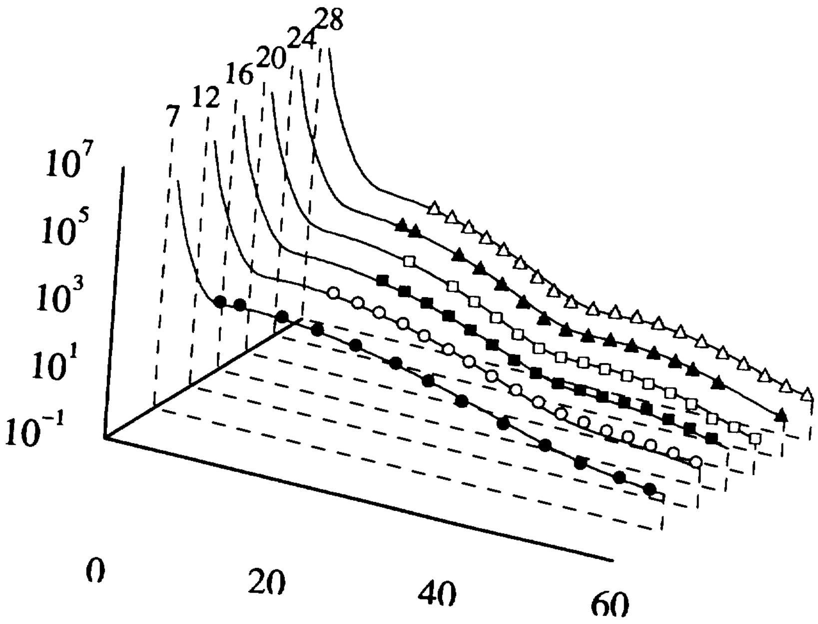

7 12 16 20 24 28
10^7
10^5
10^3
10^1
10^-1
0
20
40
60

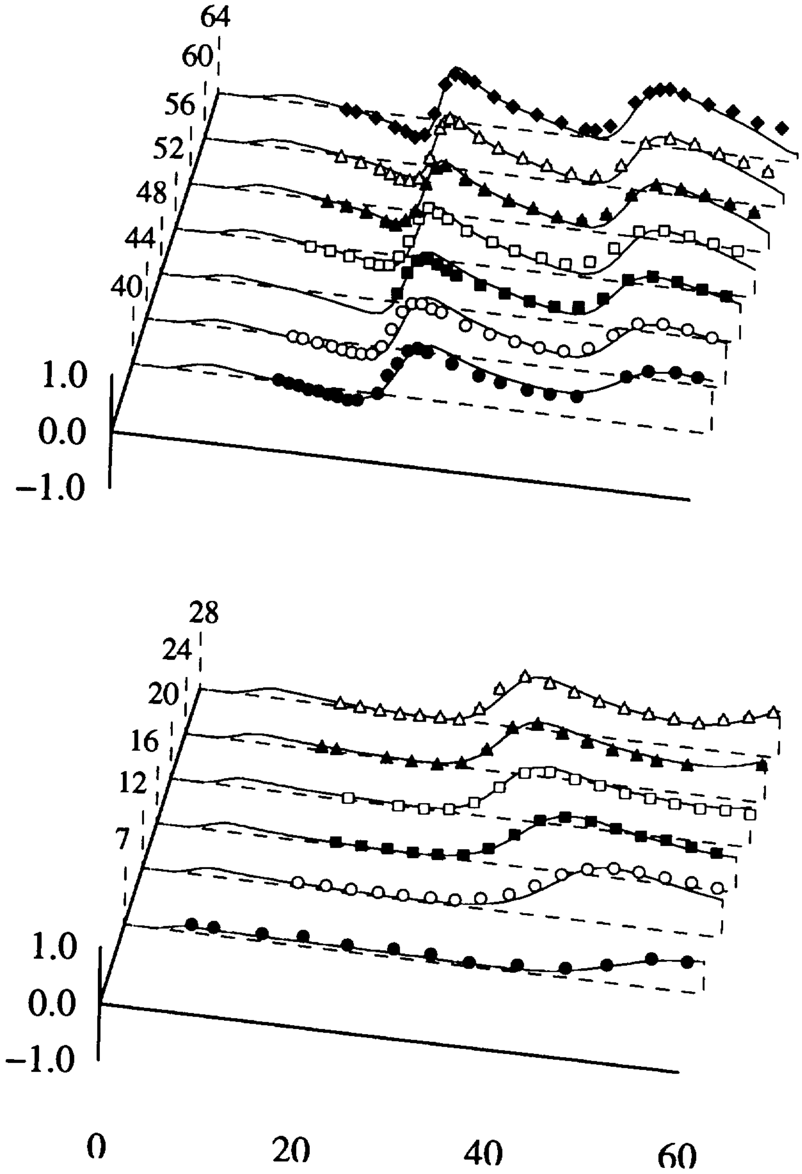

64
60
56
52
48
44
40
1.0
0.0
−1.0
28
24
20
16
12
7
1.0
0.0
−1.0
0
20
40
60

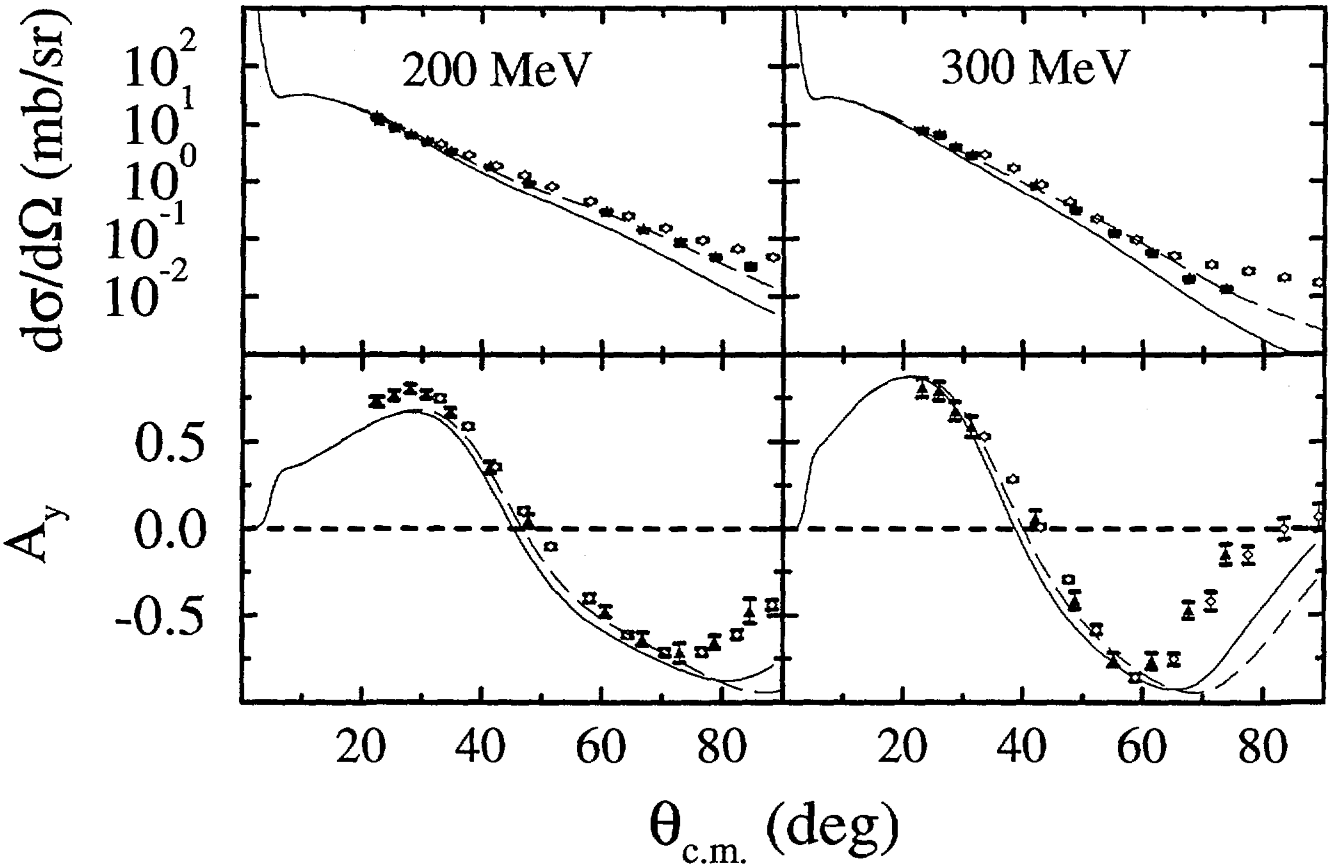

200 MeV
300 MeV
dσ/dΩ (mb/sr)
10^2
10^1
10^0
10^-1
10^-2
A_y
0.5
0.0
-0.5
20
40
60
80
θ_c.m. (deg)

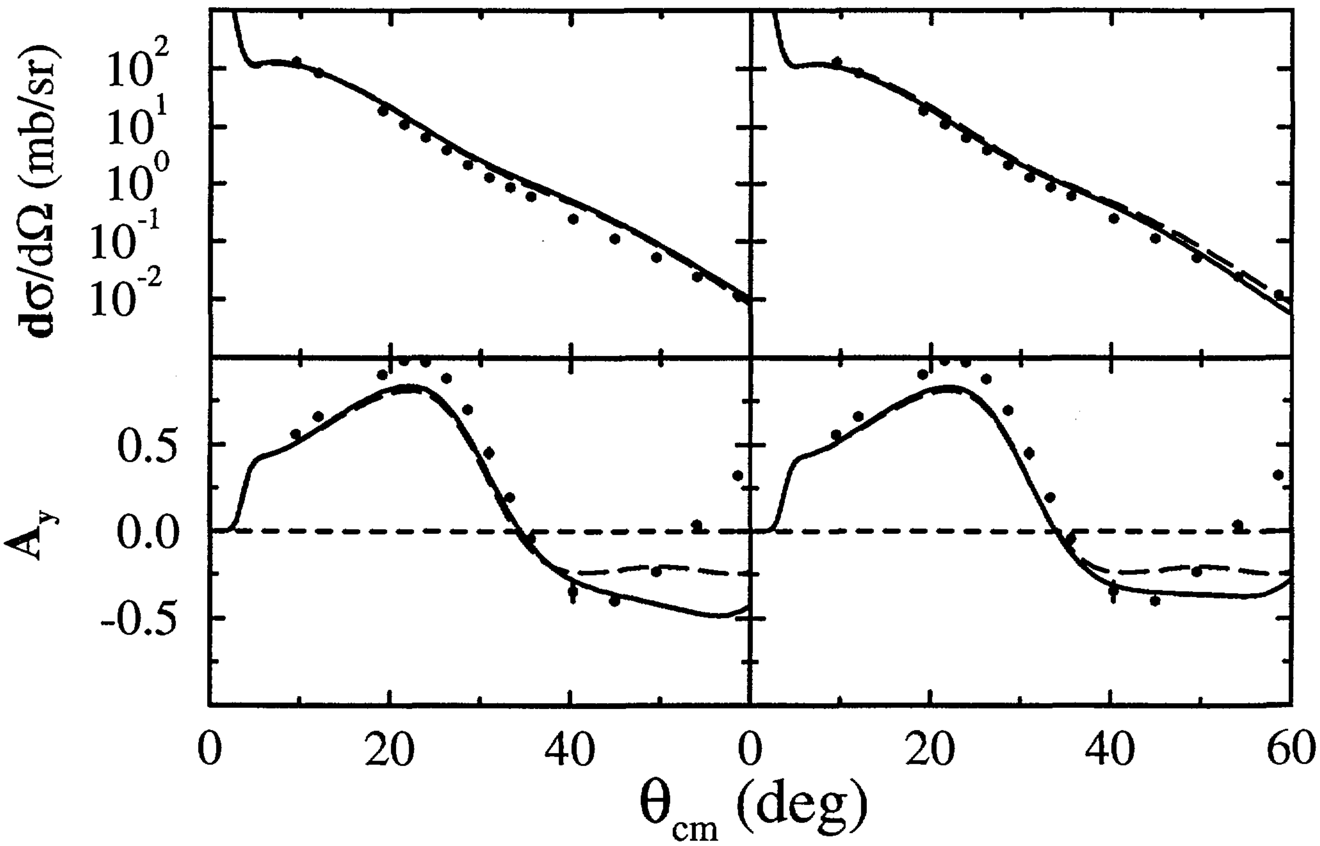

dσ/dΩ (mb/sr)
10^2
10^1
10^0
10^{-1}
10^{-2}
A_y
0.5
0.0
-0.5
0
20
40
0
20
40
60
θ_{cm} (deg)

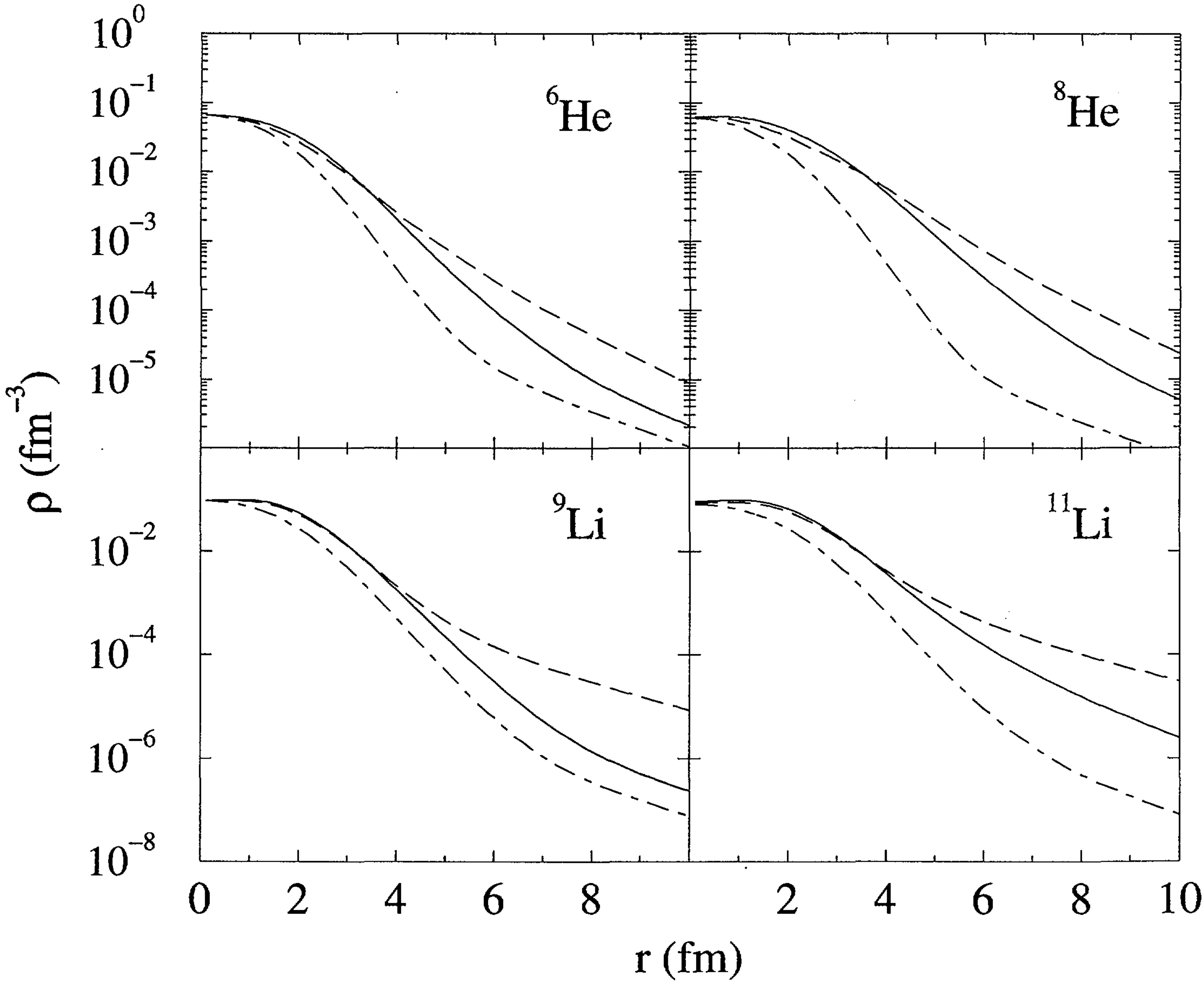

10^0
10^{-1}
10^{-2}
10^{-3}
10^{-4}
10^{-5}
10^{-6}
10^{-8}
^{6}He
^{8}He
^{9}Li
^{11}Li
ρ (fm^{-3})
0
2
4
6
8
10
r (fm)

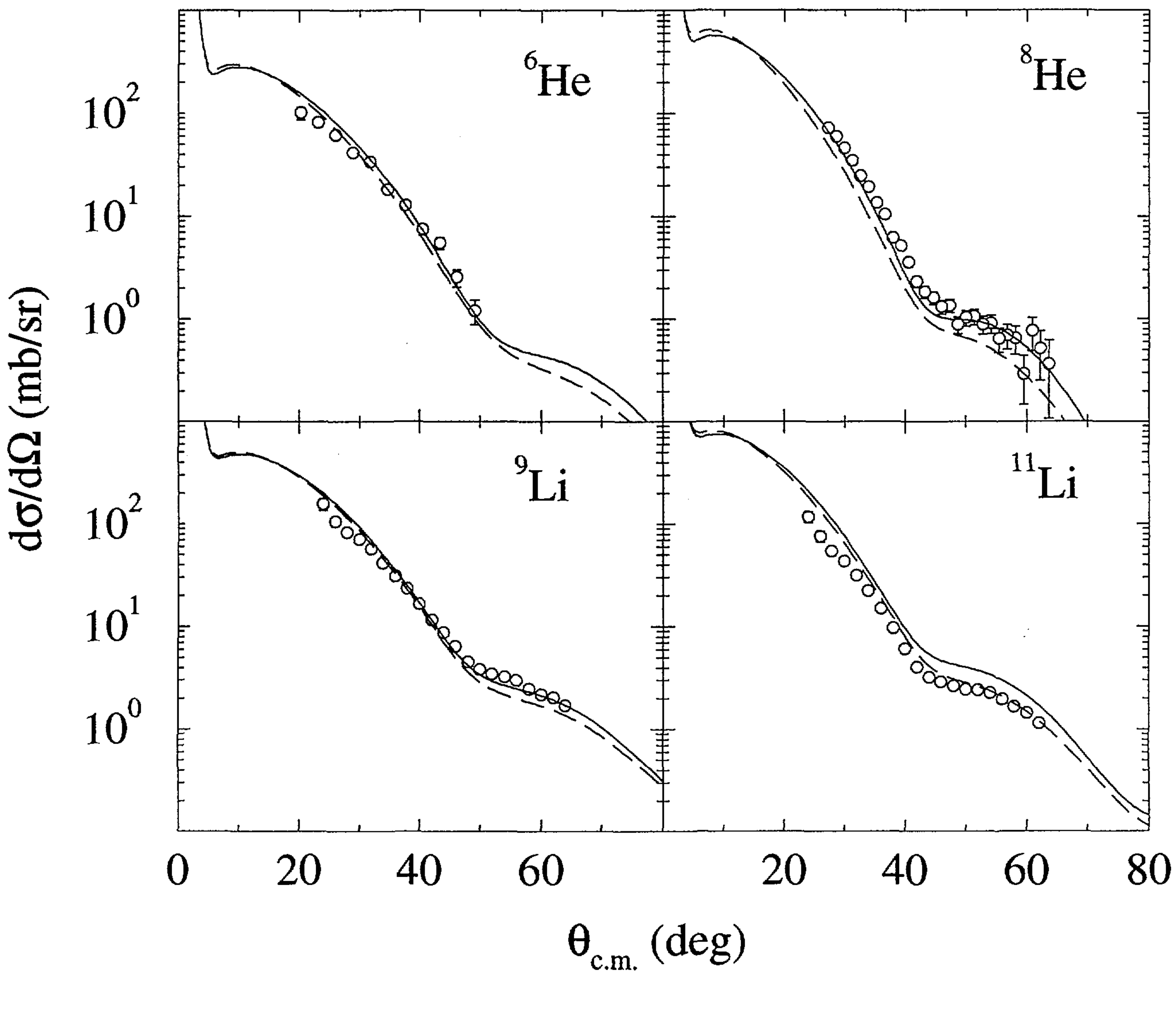

^{6}He
^{8}He
^{9}Li
^{11}Li
$d\sigma/d\Omega$ (mb/sr)
10^2
10^1
10^0
0
20
40
60
80
$\theta_{c.m.}$ (deg)

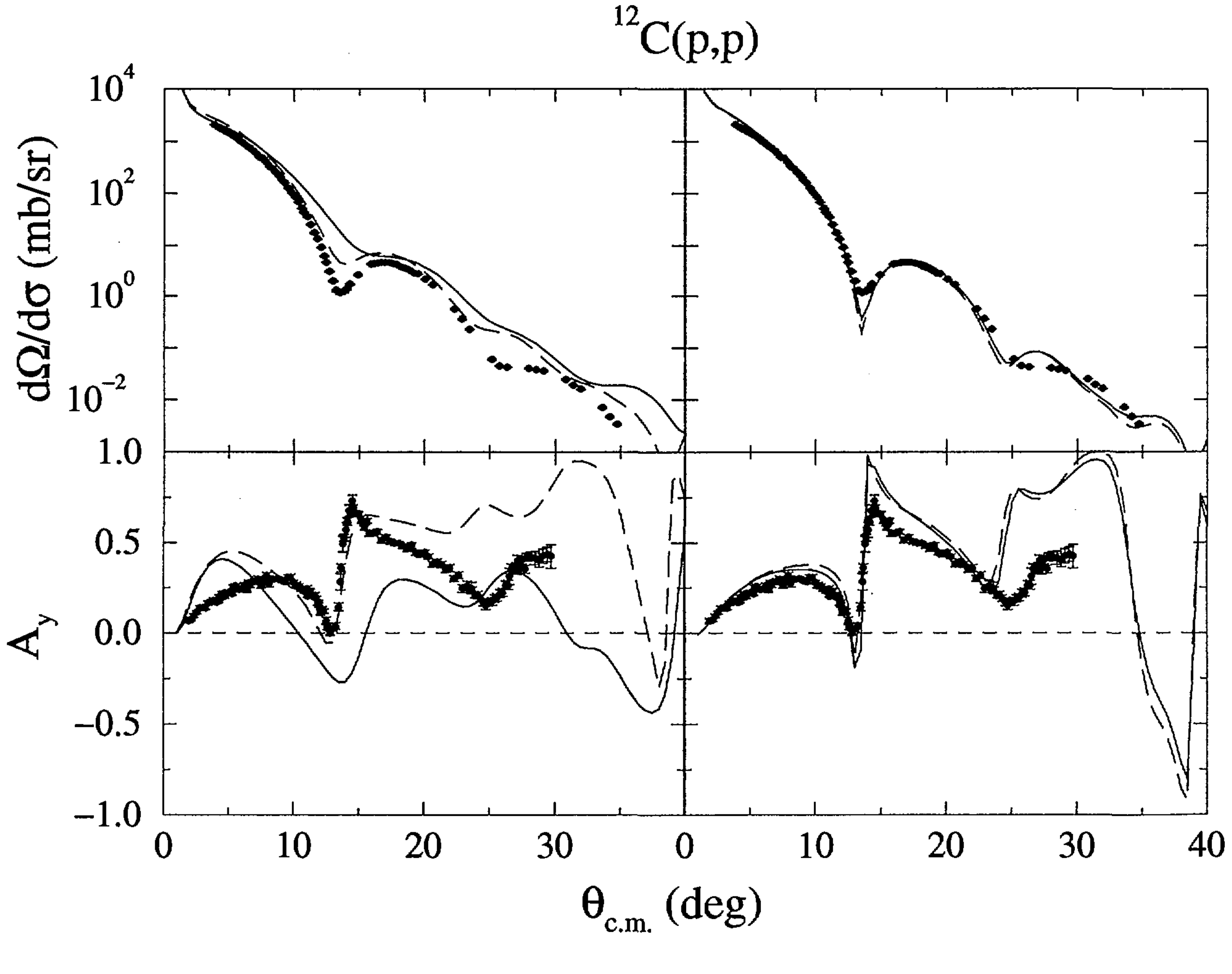

^{12}C(p,p)
dΩ/dσ (mb/sr)
A$_y$
θ$_{c.m.}$ (deg)